Entropy studies for the damped and the undamped Jaynes-Cummings model

1998 J. Phys. A: Math. Gen. 31 3395

(http://iopscience.iop.org/0305-4470/31/15/006)

J. Phys. A: Math. Gen. **31** (1998) 3395–3416. Printed in the UK PII: S0305-4470(98)89074-4

Entropy studies for the damped and the undamped Jaynes–Cummings model

F Farhadmotamed, A J van Wonderen and K Lendi

Institute of Physical Chemistry, University of Zurich, Winterthurerstrasse 190, CH-8057 Zurich, Switzerland

Received 7 November 1997, in final form 16 January 1998

Abstract. On the basis of a representation in terms of photon-number states we derive an analytically solvable set of ordinary differential equations for the matrix elements of the density operator belonging to the Jaynes–Cummings model. We allow for atomic detuning, spontaneous emission, and cavity damping, but we do not take into account the presence of thermal photons. The exact results are employed to perform a careful investigation of the evolution in time of atomic inversion and von Neumann entropy. A factorization of the initial density operator is assumed, with the privileged field mode being in a coherent state. We invoke the mathematical notion of maximum variation of a function to construct a measure for entropy fluctuations. In the undamped case the measure is found to increase during the first few revivals of Rabi oscillations. Hence, the influence of the surroundings on the atom does not decrease monotonically from time zero onwards. A further non-Markovian feature of the dynamics is given by the strong dependence of our measure on the initial atomic state, even for times at which damping brings about irreversible decay. For weak damping and high initial energy density the atomic evolution exhibits a crossover between quasireversible revival dynamics and irreversible Markovian decay. During this stage the state of maximum entropy acts as an attractor for the trajectories in atomic phase space. Subsequently, all trajectories follow a unique route to the atomic ground state, for which the off-diagonals of the atomic density matrix equal zero. From our entropy studies one learns what kind of difficulties must be overcome in establishing formulae for entropy production, the use of which is not limited to semigroup-induced dynamics.

1. Introduction

Quantum processes of a dissipative nature can be described in a fundamental and mathematically rigorous manner by coupling the quantum system under consideration to a second system, usually called the reservoir [1, 2]. All basic constraints of quantum mechanics are obeyed, because the density operator for the system and reservoir evolves with the von Neumann equation. The latter gives rise to a unitary time evolution. The dynamical behaviour of the quantum system alone is of nonunitary character in general. It is dictated by the reduced density operator, which is obtained by taking a partial trace of the full density operator. Depending on the number of degrees of freedom contained in the reservoir, the dynamics of the open quantum system is of quasiperiodic or irreversible type.

The reduced density operator does not only give access to all observables, but also allows us to consider the entropy of the dissipative quantum system. In computing this quantity, preference must be given to the von Neumann functional [3]. It can be constructed from first principles [4], and has been shown to serve as an important link between quantum mechanics and statistical physics [5–8]. For example, inspired by the second law of thermodynamics

0305-4470/98/153395+22$19.50

[9], one can employ the von Neumann entropy to make statements on the subject of quantum irreversibility. Theorems on monotonic evolution of entropy [10] and formulae for entropy production have been established [11]. Of course, one is not obliged to consider only the von Neumann entropy [12].

In [10, 11] it has been assumed that the reduced density operator satisfies a master equation of Markovian type [13, 14]. If one wishes to refrain from this assumption, then it becomes much harder to derive principles that are akin to the second law of thermodynamics. Mathematically rigorous proposals for entropy production, which can be applied to cases of non-Markovian dynamics, have not been formulated as yet. In order to survey the difficulties that are encountered in extending the existing concepts, one should analyse the behaviour of the von Neumann entropy for a quantum evolution of truly non-Markovian character. Owing to its famous dynamics of collapse and revival [15], the Jaynes–Cummings model [16, 17] offers such an evolution. A two-level atom constitutes the dissipative quantum system, so the reduced density operator acts on a Hilbert space of finite dimension. For the Jaynes–Cummings model, several studies of the von Neumann entropy and related quantities have been published [18–23]. With one exception [24], the entropy has only been plotted for initial atomic states that are pure.

The programme described above should also be carried out for a damped version of the Jaynes–Cummings model. In doing so one has the opportunity to study the von Neumann entropy for an evolution that includes both a quasireversible and a fully irreversible stage. Our aim is perfectly feasible, because in a recent paper the Jaynes–Cummings model with cavity damping has been solved exactly [25]. At zero temperature and in the absence of atomic detuning, analytic expressions have been presented for all matrix elements of the full density operator in number-state representation. A mathematical limit has been put forward in which the atomic density matrix converges to the state of maximum entropy. The last result represents an additional motivation to explore the dynamics of the damped case in some detail. We wish to find out if, for physically relevant parameter choices, the atomic entropy can indeed take on its maximum value during a longer time span. In fact, we shall see that the state of maximum entropy may act as an attractor in atomic phase space. As in the literature, this state will also be called the central state.

We give a short overview of our paper. In section 2 we develop all necessary analytical tools for studying the von Neumann entropy. We also demonstrate that in the presence of spontaneous emission and atomic detuning the Jaynes–Cummings model with cavity damping can be solved by adopting the strategy of [25]. A measure for entropy variations is constructed. It is evaluated analytically for a reference process of Markovian type. Plots of the atomic inversion and von Neumann entropy are presented in section 3. We have chosen to keep the number of plots to a minimum, so that each case can be discussed carefully. Finally, in section 4 the main conclusions of this paper are summarized.

2. Solution of the model

Working within a fully quantum-mechanical context, we are going to examine the evolution in time of a motionless two-level atom that, owing to the use of an optical resonator, interacts with a single mode of the quantized electromagnetic (em) radiation field. The dynamical behaviour of the composite system of atom (A) and field (F) is described by the density operator $\rho(t)$, which acts on the Hilbert space $\mathcal{H}_A \otimes \mathcal{H}_F$. The following Markovian master equation is adopted [1]

$$\frac{\mathrm{d}\rho(t)}{\mathrm{d}t} = \mathcal{L}_1[\rho(t)] + \kappa\mathcal{L}_2[\rho(t)] + \gamma\mathcal{L}_3[\rho(t)] \tag{1}$$

where operators $\mathcal{L}_1$, $\mathcal{L}_2$, and $\mathcal{L}_3$ are defined as

$$\mathcal{L}_1[\rho] = -\mathrm{i}[H, \rho] \tag{2}$$

$$H = \sigma_+ \otimes a + \sigma_- \otimes a^\dagger + \Delta(i_+ \otimes \mathbb{1} - i_- \otimes \mathbb{1}) \tag{3}$$

$$\mathcal{L}_2[\rho] = 2(\mathbb{1}_2 \otimes a)\rho(\mathbb{1}_2 \otimes a^\dagger) - (\mathbb{1}_2 \otimes a^\dagger a)\rho - \rho(\mathbb{1}_2 \otimes a^\dagger a) \tag{4}$$

$$\mathcal{L}_3[\rho] = 2(\sigma_- \otimes \mathbb{1})\rho(\sigma_+ \otimes \mathbb{1}) - (i_+ \otimes \mathbb{1})\rho - \rho(i_+ \otimes \mathbb{1}) - \Gamma[(i_+ \otimes \mathbb{1})\rho(i_- \otimes \mathbb{1}) + (i_- \otimes \mathbb{1})\rho(i_+ \otimes \mathbb{1})]. \tag{5}$$

The excited state and the ground state spanning the atomic Hilbert space have been represented by the vectors $\hat{e}_1 = (1, 0)^T$ and $\hat{e}_2 = (0, 1)^T$, respectively. Each atomic operator has been written as a linear combination of four matrices, given by

$$i_+ = \begin{pmatrix} 1 & 0 \\ 0 & 0 \end{pmatrix} \qquad i_- = \begin{pmatrix} 0 & 0 \\ 0 & 1 \end{pmatrix} \qquad \sigma_+ = \begin{pmatrix} 0 & 1 \\ 0 & 0 \end{pmatrix} \qquad \sigma_- = \begin{pmatrix} 0 & 0 \\ 1 & 0 \end{pmatrix}. \tag{6}$$

The creation and annihilation operators belonging to the privileged cavity mode have been denoted by $a^\dagger$ and a, respectively.

The Hamiltonian H models the interaction between the atom and field mode in the absence of energy losses. The rotating-wave and electric-dipole approximations have been employed. We have moved to the interaction picture and taken into account the fact that the frequency ω_A of the atomic transition may differ from the frequency ω_F of the privileged mode. As a consequence, expression (3) includes contributions that are proportional to the detuning parameter $\Delta = (\omega_A - \omega_F)/(2g)$, where g stands for the coupling constant of the Jaynes–Cummings Hamiltonian $H(\Delta = 0)$. Equation (1) has been divided by g so as to make time t dimensionless, as well as parameters κ and γ. The latter determine the strength of cavity damping and atomic damping, respectively. In specifying the associated operators $\mathcal{L}_2$ and $\mathcal{L}_3$ we have assumed that the cavity does not contain any thermal photons.

On the basis of expression (5) the Bloch equations can be derived. The transverse and longitudinal relaxation constants come out as $\gamma_\perp = \gamma(1 + \Gamma)$ and $\gamma_\parallel = 2\gamma$, respectively. Thus master equation (1) preserves the trace, the self-adjointness, and the positivity of the initial density operator $\rho(t = 0)$ as long as parameters κ, γ, and Γ do not become negative [26]. The factorization

$$\rho(t = 0) = \rho_A \otimes \rho_F \tag{7}$$

will be employed throughout this paper. In order to find out how the initial atomic state ρ_A evolves in time we have to evaluate the atomic density matrix $\rho_A(t)$, the entries of which read

$$\rho_A(t)_{ij} = \sum_{n=0}^{\infty} \langle \hat{e}_i \otimes n | \rho(t) | \hat{e}_j \otimes n \rangle \tag{8}$$

with $i, j = 1, 2$. In carrying out the partial trace over Hilbert space $\mathcal{H}_F$ we have chosen the photon-number states $\{|n\rangle\}_{n=0}^{\infty}$ as an orthonormal basis.

2.1. Undamped case

If damping parameters κ and γ equal zero, equation (1) can be solved with the help of two identities:

$$\begin{aligned} \exp(\mathrm{i}Ht)|\hat{e}_1 \otimes n\rangle &= A_n(t)|\hat{e}_1 \otimes n\rangle + B_n(t)|\hat{e}_2 \otimes (n+1)\rangle \\ \exp(\mathrm{i}Ht)|\hat{e}_2 \otimes n\rangle &= A^*_{n-1}(t)|\hat{e}_2 \otimes n\rangle + B_{n-1}(t)|\hat{e}_1 \otimes (n-1)\rangle. \end{aligned} \tag{9}$$

We have abbreviated

$$\begin{aligned} A_n(t) &= \cos(\Omega_n t) + \mathrm{i}\Delta\Omega_n^{-1}\sin(\Omega_n t) \\ B_n(t) &= \mathrm{i}(n+1)^{1/2}\Omega_n^{-1}\sin(\Omega_n t) \end{aligned} \tag{10}$$

and defined a Rabi frequency $\Omega_n = (n + \Delta^2 + 1)^{1/2}$. Note that function $B_{-1}(t)$ is identical to zero. In proving equations (9) one should exploit the fact that for each integer n a simple representation for operator H^n exists [27].

Upon substituting the relation $\rho(t) = \exp(-\mathrm{i}Ht)(\rho_A \otimes \rho_F)\exp(\mathrm{i}Ht)$ into (8) and making use of identities (9), one arrives at the following result for the atomic density matrix

$$\begin{aligned} \rho_A(t)_{11} = \sum_{n=0}^{\infty}[&\rho_{A,11}\rho_{F,n,n}A_n(t)A_n^*(t) + \rho_{A,12}\rho_{F,n,n+1}A_n^*(t)B_n(t) \\ &+\rho_{A,12}^*\rho_{F,n+1,n}A_n(t)B_n^*(t) + \rho_{A,22}\rho_{F,n+1,n+1}B_n(t)B_n^*(t)] \\ \rho_A(t)_{12} = \sum_{n=0}^{\infty}[&\rho_{A,12}\rho_{F,n,n}A_{n-1}^*(t)A_n^*(t) + \rho_{A,11}\rho_{F,n+1,n}A_{n+1}^*(t)B_n(t) \\ &-\rho_{A,22}\rho_{F,n+1,n}A_{n-1}^*(t)B_n(t) - \rho_{A,12}^*\rho_{F,n+2,n}B_n(t)B_{n+1}(t)]. \end{aligned} \tag{11}$$

The two remaining elements can be obtained with the help of the relations $\rho_A(t)_{22} = 1 - \rho_A(t)_{11}$ and $\rho_A(t)_{21} = \rho_A(t)_{12}^*$, which follow from the constraints $\mathrm{Tr}\,\rho(t) = 1$ and $\rho(t)^\dagger = \rho(t)$. The notation $\langle m|O|n\rangle = O_{m,n}$ has been introduced, where O denotes a field operator.

The undamped case has the drawback that it is difficult to make a mathematical statement on the asymptotic behaviour of the atomic density matrix. On the other hand, if we take as an initial condition for the field $\rho_F = |\alpha\rangle\langle\alpha|$, with $|\alpha\rangle = \exp(-|\alpha|^2/2 + \alpha a^\dagger)|0\rangle$ a coherent state, then for large times and large coherence parameter α the trigonometric factors in (11) merely give rise to oscillations of modest amplitude [28]. Accordingly, the atomic density matrix never differs much from the time average

$$\bar{\rho}_A = \lim_{T\to\infty}\frac{1}{T}\int_0^T \mathrm{d}t\,\rho_A(t). \tag{12}$$

We recall that the asymptotic regime is preceded by the well known dynamics of collapse and revival in the Rabi oscillations of matrix elements (11) [15].

In computing an off-diagonal of matrix (12) one does not meet integrands other than $\exp(\mathrm{i}at)$, with a real and nonzero. Hence, only the diagonals differ from zero. If the coherence parameter α is chosen to be real and large, then the corresponding series can be calculated analytically. We utilize Stirling's representation of a factorial and subsequently replace the summation by an integral. It is important to perform a cut-off at low photon numbers because our integration interval should not contain any singular points [25]. Application of the saddle-point method then leads to

$$\bar{\rho}_{A,11} = \tfrac{1}{2} + [(\rho_{A,11} - \tfrac{1}{2})\Delta/\alpha + \mathrm{Re}\,\rho_{A,12}](\Delta/\alpha)(1 - \Delta^2/\alpha^2) - \rho_{A,22}\Delta^2/(2\alpha^4) + \mathcal{O}(\alpha^{-5}). \tag{13}$$

In the case in which $\alpha^2 \geqslant 25$ and $|\Delta| \leqslant 2$, the above expansion matches the numerical result for $\bar{\rho}_{A,11}$ very well; the absolute error is always less than 10^{-2}. For zero detuning the right-hand side of (13) equals $\frac{1}{2}$, whereas an exact computation yields $\bar{\rho}_{A,11} - \frac{1}{2} = (\rho_{A,11}/2 - \frac{1}{2})\exp(-\alpha^2)$. The latter result practically equals zero for α large.

2.2. Damped case

We decompose the density operator for the atom and field according to

$$\rho(t) = i_+ \otimes \rho_1(t) + \sigma_- \otimes \rho_2(t) + \sigma_+ \otimes \rho_3(t) + i_- \otimes \rho_4(t) \tag{14}$$

and evaluate, on the basis of master equation (1), the time derivatives of all matrix elements of the field operators $\{\rho_j(t)\}$, opting for a number-state representation. From the ensuing equations of motion the following system can be extracted

$$\frac{\mathrm{d}}{\mathrm{d}t}\boldsymbol{v}(t;m,n) = \mathbf{A}(m,n)\boldsymbol{v}(t;m,n) + 2\kappa\mathbf{S}(m,n)\boldsymbol{v}(t;m+1,n+1) \tag{15}$$

where integers m and n run from zero to infinity.

The new vector is given by

$$\boldsymbol{v}(t;m,n) = [\rho_1(t)_{m,n}, \rho_2(t)_{m+1,n}, \rho_3(t)_{m,n+1}, \rho_4(t)_{m+1,n+1}]^T. \tag{16}$$

Matrix $\mathbf{A}$ can be found via the prescriptions

$$\begin{aligned}
&\mathbf{A}(m,n)_{kl} = \mathbf{A}(m,n)_{lk} \\
&\mathbf{A}(m,n)_{11} = -\kappa(m+n) - 2\gamma \\
&\mathbf{A}(m,n)_{22} = \mathbf{A}(m,n)^*_{33} = -\kappa(m+n+1) - \gamma(1+\Gamma) + 2\mathrm{i}\Delta \\
&\mathbf{A}(m,n)_{44} = -\kappa(m+n+2) \\
&\mathbf{A}(m,n)_{12} = \mathbf{A}(m,n)_{34} = -\mathrm{i}(m+1)^{1/2} \\
&\mathbf{A}(m,n)_{13} = \mathbf{A}(m,n)_{24} = \mathrm{i}(n+1)^{1/2} \\
&\mathbf{A}(m,n)_{14} = \mathbf{A}(m,n)_{23} = 0.
\end{aligned} \tag{17}$$

For the second matrix in (15) one has

$$\begin{aligned}
&\mathbf{S}(m,n)_{11} = (m+1)^{1/2}(n+1)^{1/2} \\
&\mathbf{S}(m,n)_{22} = (m+2)^{1/2}(n+1)^{1/2} \\
&\mathbf{S}(m,n)_{33} = (m+1)^{1/2}(n+2)^{1/2} \\
&\mathbf{S}(m,n)_{44} = (m+2)^{1/2}(n+2)^{1/2} \\
&\mathbf{S}(m,n)_{41} = \gamma/\kappa.
\end{aligned} \tag{18}$$

All other elements of matrix $\mathbf{S}(m,n)$ are equal to zero.

Evaluation of the atomic density matrix by means of equation (8) requires that the solutions for vector $\boldsymbol{v}(t;m,n)$ and matrix element $\rho_3(t)_{0,0}$ be available. Therefore we need to supplement set (15) with two more equations of motion, given by

$$\begin{pmatrix} \mathrm{d}/\mathrm{d}t + \gamma(1+\Gamma) + 2\mathrm{i}\Delta & \mathrm{i} \\ \mathrm{i} & \mathrm{d}/\mathrm{d}t + \kappa \end{pmatrix} \begin{pmatrix} \rho_3(t)_{0,0} \\ \rho_4(t)_{1,0} \end{pmatrix} = \begin{pmatrix} 2\kappa\boldsymbol{v}(t;1,0)_3 \\ 2\gamma\boldsymbol{v}(t;1,0)_1 + 2^{3/2}\kappa\boldsymbol{v}(t;1,0)_4 \end{pmatrix}. \tag{19}$$

In [25] it has been demonstrated that the ordinary first-order differential equations (15) and (19) can be solved by means of Laplace transformation and iteration. For the case of $\gamma = \Delta = 0$ explicit expressions for all matrix elements $\rho_j(t)_{m,n}$ have been obtained. The density operator $\rho(t)$ has been shown to converge to the state of lowest energy $i_- \otimes |0\rangle\langle 0|$, as time t tends to infinity.

2.3. Entropy

Knowledge of density matrix $\rho_A(t)$ gives us access to the von Neumann entropy [3, 6] of the atom. It is defined as

$$S_A(t) = S[\rho_A(t)] \qquad S[\rho] = -k_B \operatorname{Tr}\{\rho \ln \rho\} \tag{20}$$

where k_B denotes Boltzmann's constant, and ρ any density operator. The non-negative functional $S[\rho]$ satisfies a uniqueness theorem. It can be constructed by proposing a set of properties that must be satisfied by any quantum entropy [4]. With the help of the von Neumann entropy one can make fundamental connections between quantum mechanics and statistical physics. First, for a large quantum system in thermodynamic equilibrium the complete formalism of statistical mechanics can be set up by applying a principle of maximum entropy to (20) [5].

Second, for a small dissipative quantum system $\mathcal{S}$, for example, a system with a Hilbert space of finite dimension, the von Neumann entropy can be employed to formulate a quantum-mechanical counterpart of the second law of thermodynamics [9]. Let us discuss this point in detail. Describing the time evolution of $\mathcal{S}$ by a density matrix $\rho_S(t)$, we assume that the relation $\rho_S(t) = \Lambda(t)\rho_S(t=0)$ is valid, where the (super-)operators $\{\Lambda(t)|t \geqslant 0\}$ form a quantum-dynamical semigroup [14]. One possibility to realize such a Markovian time evolution consists of coupling $\mathcal{S}$ to a large reservoir, and subsequently taking the weak-coupling limit [13].

If no work is carried out, the quantum formulation of the second law reads

$$\sigma(t) = \frac{\mathrm{d}}{\mathrm{d}t}(S[\rho_S(t)] - T^{-1} \operatorname{Tr}\{\rho_S(t) H_S\}) \tag{21}$$

where H_S denotes the Hamiltonian of $\mathcal{S}$, and T the temperature of the reservoir. Quantity $\sigma(t)$, which is commonly called the entropy production, should be non-negative for all times. In the case in which $\rho_S(t)$ converges for large times to the Gibbs state $Z^{-1}\exp[-H_S/(k_B T)]$, with $Z = \operatorname{Tr}\{\exp[-H_S/(k_B T)]\}$, (21) can be written as [11]

$$\sigma(t) = -k_B \frac{\mathrm{d}}{\mathrm{d}t} R[\Lambda(t)\rho_S(0), \Lambda(\infty)\rho_S(0)]. \tag{22}$$

We have introduced the relative entropy

$$R[\rho_1, \rho_2] = \operatorname{Tr}\{\rho_1(\ln \rho_1 - \ln \rho_2)\} \tag{23}$$

with ρ_1 and ρ_2 arbitrary density operators. One can prove [29] that for all completely positive quantum-dynamical semigroups $\{\Lambda(t)|t \geqslant 0\}$, with $\Lambda(\infty)\rho_S(0)$ a well-defined operator, the right-hand side of (22) is indeed non-negative. Thus the last identity constitutes a quantum version of the second law of thermodynamics. Observe that matrix $\rho_1 \ln \rho_2$ becomes divergent if ρ_2 approaches a pure state.

For quantum dissipative processes, which must be described on the basis of a non-Markovian master equation, it is impossible to formulate a principle that is directly analogous to the second law of thermodynamics. To map all the difficulties one may encounter in tackling this problem, we should examine the behaviour of the von Neumann entropy for one specific quantum system, the dynamical behaviour of which is of a truly non-Markovian nature. Because of the collapses and revivals in its Rabi oscillations [15], the atomic density matrix $\rho_A(t)$ of the Jaynes–Cummings model seems to be an ideal candidate.

The above choice has a further advantage. For large times and nonzero damping parameter κ or γ, the density matrix exponentially decays to the state of lowest energy, so that the entropy converges to zero. We shall therefore be in a position to study a crossover between non-Markovian and Markovian dynamics. As pointed out earlier, for the undamped

case convergence does not take place. However, if the field starts from a coherent state with a large coherence parameter, then the atom eventually stays in the vicinity of the central state $\frac{1}{2}\mathbb{1}_2$, as follows from (13). Consequently, variations of entropy $S_A(t)/k_B$ will be confined to a small interval that lies directly below the maximum entropy value of $\ln 2$.

As we shall see in section 3, the atomic entropy $S_A(t)$ is a continuous function of time that may fluctuate a lot. If we were to characterize its behaviour in detail, for instance by specifying all of its extrema, then we would be confronted with a huge amount of data, and hence lose the overview. What we shall do is select a number of time intervals $[t_1, t_2]$ of equal length, and find out for each of these how strong fluctuations are. This task can be carried out by evaluating a quantity called the maximal variation of a function. It is defined as

$$\psi(t_1, t_2) = \int_{t_1}^{t_2} \mathrm{d}t \left[\frac{\mathrm{d}S_A(t)}{\mathrm{d}t}\right]^2. \tag{24}$$

For a closed quantum system the time evolution of the density operator is determined by unitary transformations, so the von Neumann entropy remains constant. In other words, any change in $S_A(t)$ must be ascribed to interaction between the two-level atom and its surroundings. The quantity $\psi(t_1, t_2)$ can be regarded as a measure for the influence that the field mode and the Markovian reservoirs exert on the two-level atom during the time interval $[t_1, t_2]$.

In discussing the behaviour of measure ψ, it is instructive to make a comparison with values that belong to a reference process. The latter should obey the requirements underlying the positivity of entropy production (22). We consider Markovian dynamics in the diagonals of the density matrix $\xi(t)$ for a two-level atom. The off-diagonal elements are kept equal to zero so as to allow for an analytical evaluation of (24). We start from the identities

$$\xi(t)_{11} = \xi(\infty)_{11} + [\xi(0)_{11} - \xi(\infty)_{11}] \exp(-\gamma_\parallel t) \tag{25}$$

and $\xi(t)_{22} = 1 - \xi(t)_{11}$, where parameters $\xi(0)_{11}$ and $\xi(\infty)_{11}$ must be elements of the interval $[0, 1]$. By choosing $\xi(0)_{11} = 1$, $\xi(\infty)_{11} = 0$, one describes spontaneous emission of a photon. The lifetime of the excited atomic level is given by $\gamma_\parallel^{-1}$.

Since matrix $\xi(\infty)$ is diagonal, the relative entropy $R[\xi(t), \xi(\infty)]$ can be calculated without any problems. Now the form (22) comes out as

$$\sigma(t) = k_B \gamma_\parallel \exp[-\gamma_\parallel t][\xi(0)_{11} - \xi(\infty)_{11}] \ln\left[\frac{\xi(t)_{11}}{1-\xi(t)_{11}} \frac{1-\xi(\infty)_{11}}{\xi(\infty)_{11}}\right]. \tag{26}$$

Function $x/(1-x)$ monotonically increases on the interval $0 \leqslant x < 1$, so for our reference process the entropy production is indeed positive. As anticipated above, it diverges if we start from, or end up, in a pure state.

Upon departing from (25) and performing an integral transformation we obtain for measure (24)

$$\begin{aligned} &\psi(t_1, t_2) = \tfrac{1}{4} k_B^2 \gamma_\parallel \{[1 - 2\xi(\infty)_{11}] I_1(u_1, u_2) + I_2(u_1, u_2)\} \\ &u_i = 2\xi(\infty)_{11} - 1 + 2[\xi(0)_{11} - \xi(\infty)_{11}] \exp(-\gamma_\parallel t_i) \end{aligned} \tag{27}$$

with $i = 1, 2$. Two integrals must be computed, namely

$$\begin{aligned} I_1(u_1, u_2) &= \int_{u_2}^{u_1} \mathrm{d}x \, \ln^2\left(\frac{1+x}{1-x}\right) \\ I_2(u_1, u_2) &= \int_{u_2}^{u_1} \mathrm{d}x \, x \ln^2\left(\frac{1+x}{1-x}\right). \end{aligned} \tag{28}$$

Boundaries u_1 and u_2 lie inside interval $[-1, 1]$. Both I_1 and I_2 can be calculated via partial integration. In the case of I_1 one encounters integral 2.728.1 of [30]. For the process of spontaneous emission the result $\psi(0, \infty) = \pi^2 k_B^2 \gamma_\parallel / 6$ is found.

3. Dynamics of the two-level atom

On the basis of the analytical solutions presented in the previous section and in [25], we shall examine the evolution in time of the atomic inversion, defined as $d(t) = [\rho_A(t)_{11} - \rho_A(t)_{22}]/2$, and the scaled von Neumann entropy $S_A(t)/k_B$. It should be emphasized that in computing all infinite series for the atomic density matrix $\rho_A(t)$, we have invoked mathematically sound truncation criteria. For the damped case these have been derived in [25]. In computing the measure ψ, defined in (24), differentiations and subsequent integrations have been performed numerically. To ensure an excellent accuracy the behaviour of each function $S_A(t)$ has been determined with great precision. For regions exhibiting strong fluctuations a resolution of 10^3 points per unit of time has been employed.

For all of our plots the initial condition $\rho(0) = \rho_A \otimes |\alpha\rangle\langle\alpha|$ has been chosen, with coherence parameter α real. Its square is equal to the mean photon number. We recall that time t has been scaled; one unit of time is given by the inverse of the coupling constant g.

3.1. Undamped case

In figures 1 and 2 functions $d(t)$ and $S_A(t)/k_B$ have been plotted for the choice $\rho_A = i_+$, $\alpha = 5$, and $\gamma = \kappa = \Delta = 0$. On the interval $0 \leqslant t \leqslant 2$ the Rabi oscillations in the inversion almost collapse, while on the interval $20 \leqslant t \leqslant 80$ one encounters two well-separated revivals. The amplitude of the Rabi oscillations attains a maximum at the so-called revival times T_n, which are found as [15] $T_n = 2n\pi(\alpha^2 + \Delta^2)^{1/2}$, with n an integer. For times larger than 100 the inversion fluctuates in an irregular manner about its average value $\bar{d}$ of zero. As observed above, convergence does not take place.

The first collapse for the inversion is accompanied by a sharp increase in entropy. One checks that at time $t = 2$ the initial pure state i_+ has practically evolved to the central state $\frac{1}{2}\mathbb{1}_2$. On the interval $2 \leqslant t \leqslant 100$ the entropy displays a very marked behaviour. The small-scale fluctuations can be ascribed to Rabi oscillations in all elements of the atomic density matrix. In contrast, the sequence of low minima at $t \approx 18$, 47, and 80 relates to dynamics in the off-diagonal $\rho_A(t)_{12}$. This matrix element governs the evolution of the induced electric-dipole moment. If it were equal to zero, then the entropy would not differ much from $\ln 2$ during a collapse. For large times the entropy plot of figure 2 has a completely irregular character. As anticipated above, the average value of the entropy lies close to $\ln 2$.

In the appendix we compute the atomic density matrix for large coherence parameter and γ, κ, Δ equal to zero. As in [28], the off-diagonal matrix element $\rho_A(t)_{12}$ is found to perform oscillations at both a high frequency of order α and a low frequency of order α^{-1}. The former oscillations are of the Rabi type, and give rise to the same kind of revival dynamics that is observed in the atomic inversion. The oscillations of low frequency bring about a very slow dynamical evolution, which also exhibits collapses and revivals. The first collapse lasts from time $t = 0$ until $t \approx 4\sqrt{2}\alpha^2$; it is this collapse of slow oscillations in matrix element $\rho_A(t)_{12}$ that underlies the large-scale oscillations in entropy, as displayed in figure 2 for $2 \leqslant t \leqslant 100$.

The amplitude of Rabi oscillations depends a lot on the initial atomic density matrix. If we choose as matrix ρ_A the mixed state $\frac{1}{2}\mathbb{1}_2$ in drawing figure 1, then the inversion

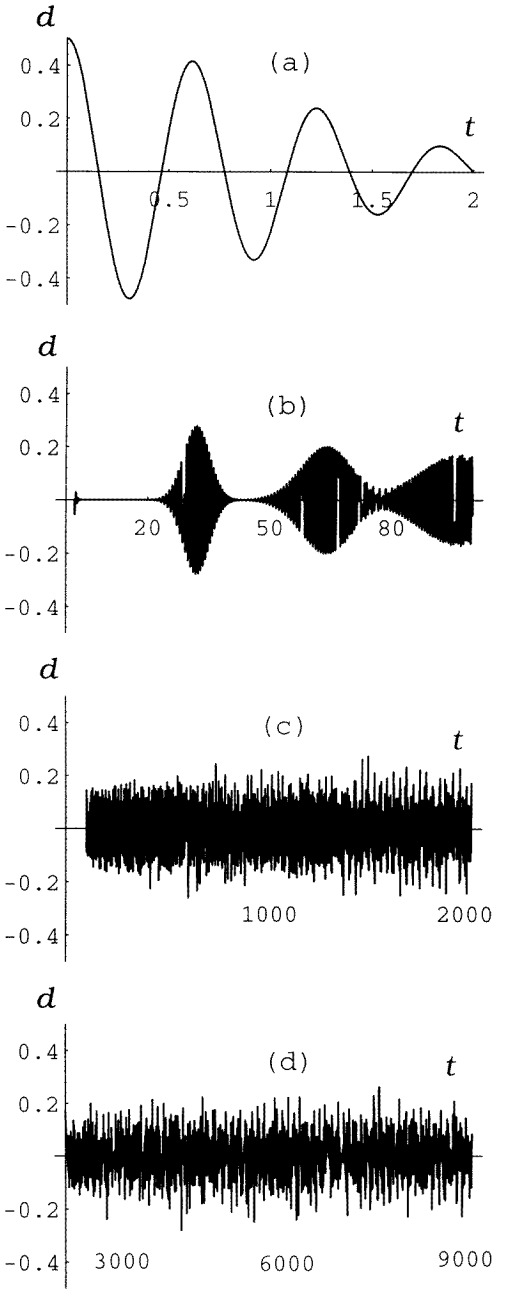

Figure 1. Time evolution of atomic inversion for $\rho_A = i_+$, $\alpha = 5$, and $\gamma = \kappa = \Delta = 0$.

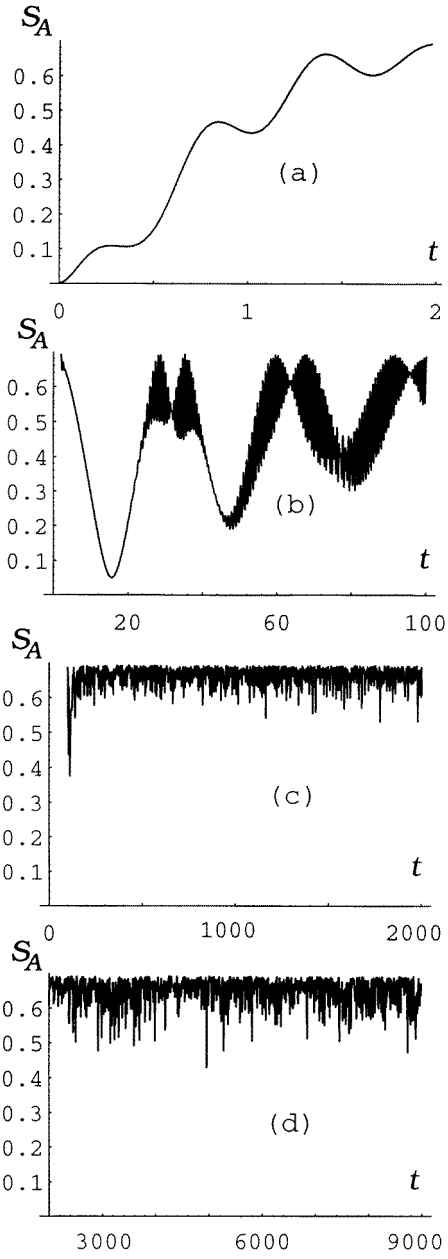

Figure 2. Time evolution of von Neumann entropy. All parameters as in figure 1.

almost remains zero. Its evolution has been monitored up to times of order 10^6. Hence, the atom remembers very well from which state it has started. Such memory effects are typical for non-Markovian processes [2]. The choice of matrix ρ_A also has a big influence on the entropy, especially as the first collapse of Rabi oscillations takes place. To illustrate

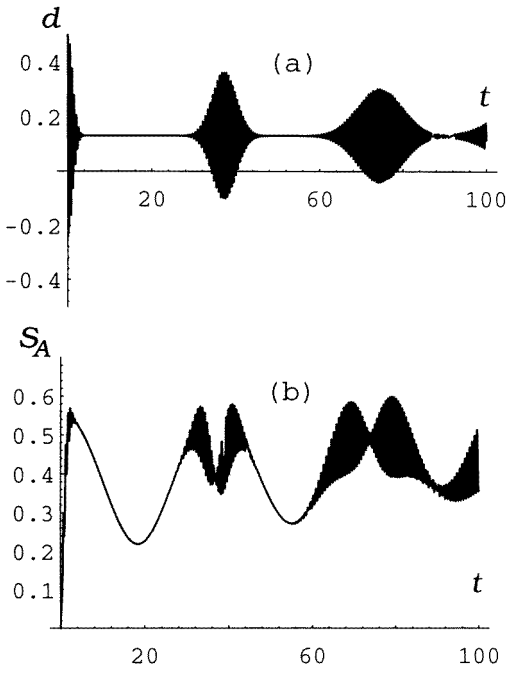

Figure 3. Time evolution of atomic inversion and von Neumann entropy for $t \leqslant 100$, $\rho_A = i_+$, $\alpha = 5$, $\Delta = 3$, and $\gamma = \kappa = 0$.

this statement we have computed measure (24) for ρ_A varying between i_+ and $\frac{1}{2}\mathbb{1}_2$, with $\rho_{A,12}$ and t_1 zero, $t_2 = T_1/5$, and all other parameters as in figure 1. We have found that ψ/k_B^2 monotonically decreases from 0.66 for the pure state to 0.01 for the central state. The decrease can be explained by observing that, apart from a few exceptions [22, 31], all initial atomic states evolve during the first collapse to the central state via a simple trajectory in phase space.

For nonzero detuning parameter, memory effects in the evolution of the two-level atom become still more pronounced. Now, not only the amplitude of Rabi oscillations, but also the time average of the inversion is affected by variations in the initial atomic state. In figure 3 we have increased Δ to 3, and taken all other parameters as in figure 1. One observes that the inversion oscillates about the value of 0.13 instead of zero. This shift can be perfectly understood on the basis of expansion (13), from which the result $\bar{d} = 0.115$ is found. For the entropy the characteristic sequence of minima is there again. As compared with the case $\Delta = 0$, the locations of the minima have moved to the right, and the first minimum is less deep [21]. Furthermore, for times smaller than 100 the entropy no longer exceeds the value of 0.6; for large times of order 10^4 the entropy fluctuates in the same irregular manner as in figure 2, and stays on average well above the value of 0.6.

As discussed in the previous section, it is useful to gain quantitative information on fluctuations in the atomic entropy. The programme described near (24) has been carried out for several parameter sets, including those covered by figures 2 and 3(*b*). A natural choice for the intervals $[t_1, t_2]$ is provided by the revival times $T_n = nT_1$, with n an integer. Starting at time $T_1/2$, we divide the time axis into successive intervals of fixed duration T_1. The quantity $\psi_n \equiv \psi[(n - \frac{1}{2})T_1, (n + \frac{1}{2})T_1]$ then delivers us the maximal variation of entropy during interval I_n containing the nth revival. Of course, integer n need not be limited by the number of revivals that really take place. Results for measure ψ_n have been collected in table 1.

Table 1. Values of measure ψ_n/k_B^2 for four choices of α and Δ. Damping parameters γ and κ are equal to zero, and for the initial atomic state the choice $\rho_A = i_+$ has been made.

n	$\alpha = 5$ $\Delta = 0$	$\alpha = 10$ $\Delta = 0$	$\alpha = 5$ $\Delta = 3$	$\alpha = 10$ $\Delta = 3$
1	5.2	5.3	3.5	4.7
2	13.0	17.9	7.7	15.4
3	13.4	35.2	7.4	30.3
4	9.6	50.4	13.6	43.1
5	7.6	56.5	13.4	47.1
6	6.2	52.8	11.0	47.3
7	5.4	44.3	8.9	45.9

The most striking fact about our data is that ψ_n does not behave monotonically as a function of n, but goes through a maximum. It is not true that the atom experiences the strongest influence from the field mode during the first revival of Rabi oscillations in the inversion. Indeed, for the two revivals, which are displayed in figure 1(b) and contained in the intervals $I_1 = [15.7, 47.1]$ and $I_2 = [47.1, 78.5]$, our measure of maximal variation increases by more than a factor of 2. For interval I_3, which no longer contains a clean revival, the measure attains its maximum. If Δ is put equal to 3, the value of the maximum remains approximately the same, but both the increase and decrease of ψ_n is spread out over more intervals I_n. This confirms the intuitive statement that in the presence of detuning the dynamic interplay between the atom and field does not change in character, but proceeds at a slower pace.

The trends described above persist if we augment the mean photon number, so that a plot of the inversion exhibits more revivals. For $\alpha = 10$ they are seven in number. From the third column of table 1 one sees that relative differences in ψ_n have become much larger. The maximum value of ψ_n now exceeds ψ_1 by more than a factor of 10. Furthermore, the position of the maximum has shifted to interval $I_5 = [282.7, 345.6]$. Inside this interval fluctuations in entropy are larger than before, because for $\alpha = 10$ the ratio $(\psi_n)_{\max}/(T_1 k_B^2)$ amounts to 0.90 instead of 0.43 for $\alpha = 5$. The foregoing data demonstrate in a quantitative manner that for higher coherence parameter α the dynamic interplay between the atom and field becomes more intense and takes up more revival times T_1. The second statement can be corroborated by investigating at which instant the atomic entropy enters its asymptotic regime of irregular fluctuation in a strip below $\ln 2$. Choosing $\Delta = 0$, we find that for $\alpha = 5$, measure ψ_n/k_B^2 stays close to the value of 5 from $n = 10$ onwards. For $\alpha = 10$ the last two figures must be replaced by 10 and $n = 20$, respectively. Note that time T_1 is proportional to α, so the asymptotic value for ratio $\psi_n/(T_1 k_B^2)$ does not depend much on the coherence parameter.

The non-monotonic behaviour of measure ψ_n as a function of n is a further sign for the fact that the Jaynes–Cummings model gives rise to a non-Markovian time evolution. To make this remark more explicit we evaluate measure ψ_n for a Markovian counterpart of the time evolution shown in figure 2. We make in (25) the choices $\xi(0)_{11} = 1$ and $\xi(\infty)_{11} = \frac{1}{2}$, and divide the time axis into intervals of length $\gamma_\parallel^{-1}/10$. From (27) we infer that measure $\psi_n \equiv \psi[n\gamma_\parallel^{-1}/10, (n+1)\gamma_\parallel^{-1}/10]$ now monotonically decreases as a function of n, with n a non-negative integer. The same conclusion is reached if intervals of length $\gamma_\parallel^{-1}/100$ or $\gamma_\parallel^{-1}$ are used. The last option, however, is rather uninteresting, because the interval $t > \gamma_\parallel^{-1}$ makes a contribution of less than 0.005 to the total measure $\psi(0, \infty)/(\gamma_\parallel k_B^2) = \ln 2$.

The initial density operator $\rho(0)$ belonging to table 1 corresponds to a pure state. Hence, the total von Neumann entropy $S(t) = -k_B \operatorname{Tr}\{\rho(t) \ln \rho(t)\}$ vanishes at all times. By the fundamental inequality $|S_A(t) - S_F(t)| \leqslant S(t)$ [32], this implies the equality $S_A(t) = S_F(t)$, so all conclusions ensuing from table 1 also hold true for the entropy $S_F(t)$ of the field mode [33]. A last important remark pertaining to table 1 concerns the order of magnitude of measure ψ_n. Its dependence on the choice of initial state is quite strong. Taking Δ equal to zero and intervals I_n as before, we compute on the basis of (11) measure ψ_n for the initial conditions $\rho(0) = \frac{1}{2}\mathbb{1}_2 \otimes |\alpha\rangle\langle\alpha|$ and $\rho(0) = i_+ \otimes |m\rangle\langle m|$, where $|m\rangle$ denotes a photon-number state. To allow for a comparison with values from table 1 parameter α is set equal to 5 and integer m equal to 25. For the first case ψ_n/k_B^2 is smaller than 0.21 for all n, whereas for the second case ψ_n/k_B^2 is constant and equal to 382.

3.2. Damped case

In the remainder of this section the damping parameter κ is chosen to be finite. The optical cavity thus becomes lossy. Detuning parameter Δ and damping parameter γ are kept equal to zero; as before, the atom is in perfect resonance with the privileged em mode and does not emit photons into other modes. If one allows for cavity damping the evolution of the atomic density matrix undergoes radical changes. This can already be seen from the fact that now the following two limits are valid

$$\lim_{\kappa\to 0}{}' \rho_A(t) = \tfrac{1}{2}\mathbb{1}_2 \tag{29}$$

$$\lim_{t\to\infty} \rho_A(t) = i_-. \tag{30}$$

Detailed proofs can be found in [25]. For limit (29) the field may start from either a coherent or a photon-number state. The prime indicates that the time, the square of the initial em energy density, and parameter κ^{-1} should be taken to infinity in such a manner that all of the ratios between these quantities remain constant and nonzero. The above results demonstrate that in the presence of cavity damping both the state of minimum energy and the state of maximum entropy may act as attractors in phase space.

To visualize the influence of cavity damping in an effective manner we set κ equal to the modest value of 0.001, and redo all of figures 1 and 2. The outcome is presented in figures 4 and 5. One can distinguish between four stages of evolution, each of which has been pictured separately. During the first stage differences with the undamped case are negligibly small. Again the Rabi oscillations of the inversion collapse, while the entropy grows from zero to its maximum value of $\ln 2$. During the second stage the entropy performs a series of relatively smooth oscillations with decreasing amplitude, thereby attaining the aforementioned maximum value at regular intervals. The dynamics of stage two is completely dominated by the collapse belonging to the slow revival dynamics in the off-diagonal $\rho_A(t)_{12}$. For the undamped case this collapse has been discussed above.

The first and second entropy minima of stage two have barely shifted as compared with figure 2(*b*), so the introduction of a modest cavity damping does not affect the large-scale oscillations in entropy. The contrary is true for the Rabi oscillations. The plot of the inversion for $2 \leqslant t \leqslant 100$ shows that the amplitude of the first revival has shrunk considerably, whereas the second revival has practically vanished. Making use of the analytical results derived in section 5 of [25], one predicts that for α large all oscillations in the atomic density matrix are damped by a factor of $\exp\{-\alpha^2[1 - \exp(-2\kappa t)]\}$, at least if product $\kappa\alpha^3$ is small. For the first and the second revivals of figure 4(*b*) one has $t \approx 31$ and $t \approx 63$, leading to damping factors of 0.22 and 0.05, respectively. With regard to

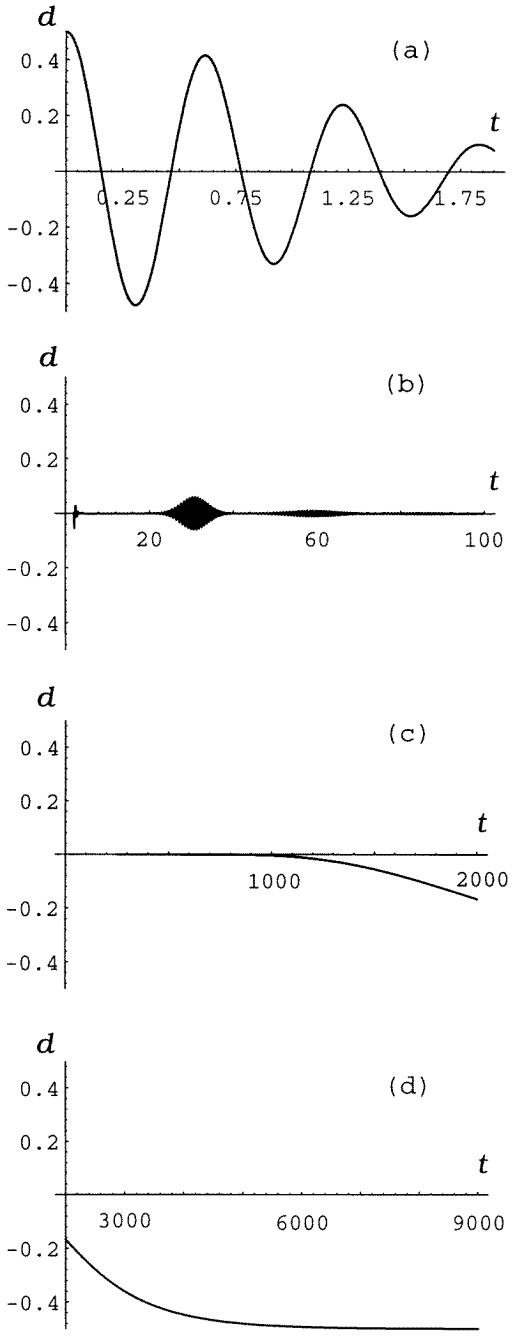

Figure 4. Time evolution of atomic inversion for $\rho_A = i_+$, $\alpha = 5$, $\kappa = 0.001$, and $\gamma = \Delta = 0$.

the large-scale oscillations, it is manifest that for $\kappa = 0.001$ and $\alpha = 5$ their behaviour does not match the predictions of the weak-damping regime. In the case in which κ equals 0.0001 the entropy plot exhibits both Rabi and large-scale oscillations. The damping factor amounts to 0.86 for the first revival time. Hence, if product $\kappa\alpha^3$ is of order 0.01, with α large, the weak-damping regime seems to produce reliable predictions.

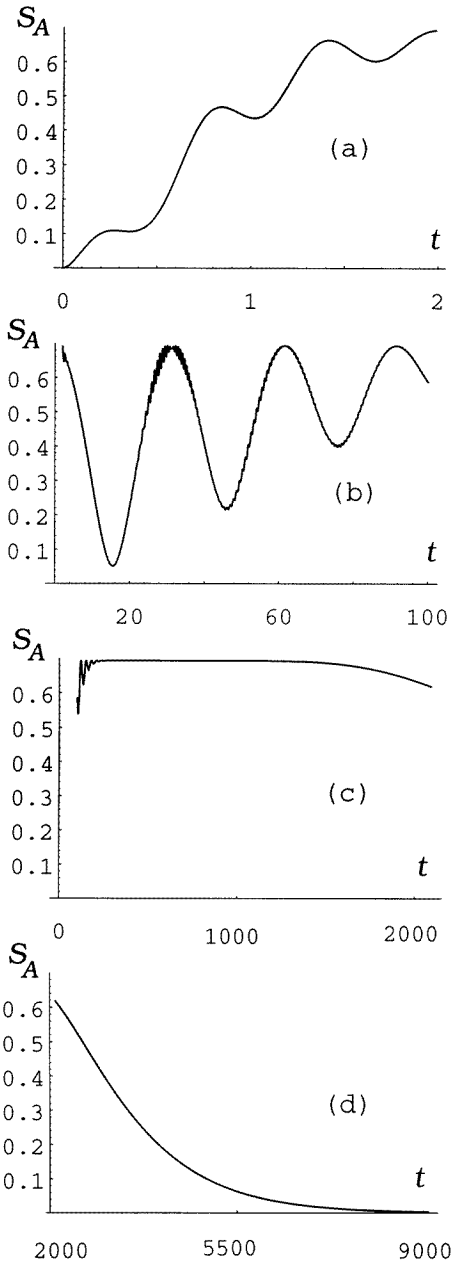

Figure 5. Time evolution of von Neumann entropy. All parameters as in figure 4.

During the third and fourth stages of the atomic evolution limits (29) and (30) come into play, respectively. Accordingly, a plot from figures 4 and 5 no longer resembles its counterpart of figures 1 and 2. For stage three the large-scale oscillations in entropy have given way to a plateau. On the interval $231 \leqslant t \leqslant 1270$ the difference $[\ln 2 - S_A(t)/k_B]$ is smaller than 10^{-3}, so the atom stays in the central state $\frac{1}{2}\mathbb{1}_2$ for a long time. One checks that parameters κ, $\kappa\alpha^4$, and κt meet the conditions accompanying limit (29) reasonably well, so indeed this limit underlies stage three. The fourth and last stage shows us a smooth

decay of the central state to the ground state i_-, as imposed by limit (30). As for the third stage, matrix element $\rho_A(t)_{12}$ remains close to zero throughout. For $t \geqslant 10\,290$ the entropy is smaller than 10^{-3}.

The dynamical behaviour displayed in figure 5 is representative for a large part of the parameter space spanned by ρ_A, α, and κ. We have checked that the four different stages of evolution can be spotted for $10 \leqslant \alpha^2 \leqslant 25$ and $0.0001 \leqslant \kappa \leqslant 0.01$; their existence does not depend on the initial atomic state. If we vary matrix ρ_A, still choosing $\alpha = 5$ and $\kappa = 0.001$, then only quantitative changes in the atomic evolution occur. For the first two stages modifications are largely identical to those observed for the undamped case. Again the amplitude of the Rabi oscillations becomes small as ρ_A approaches the central state. With regard to stage three, the length and location of the plateau of maximum entropy may change somewhat. For $\rho_{A,11} = 0.6$ and $\rho_{A,12} = 0.1 + \mathrm{i}0.2$ it runs from $t = 177$ to $t = 1261$. The exponential decay of stage four hardly depends on the initial atomic state. For the last-mentioned choice the entropy dives below the value of 10^{-3} at $t = 10\,280$ instead of $t = 10\,290$ for the initial condition $\rho_A = i_+$.

By augmenting damping parameter κ we bring about qualitative changes in the atomic evolution. Figure 6 contains an entropy plot for $\alpha = 5$ and $\kappa = 0.01$. The atom is in the central state initially. This explains why, up to time $t = 2$, the entropy does not differ

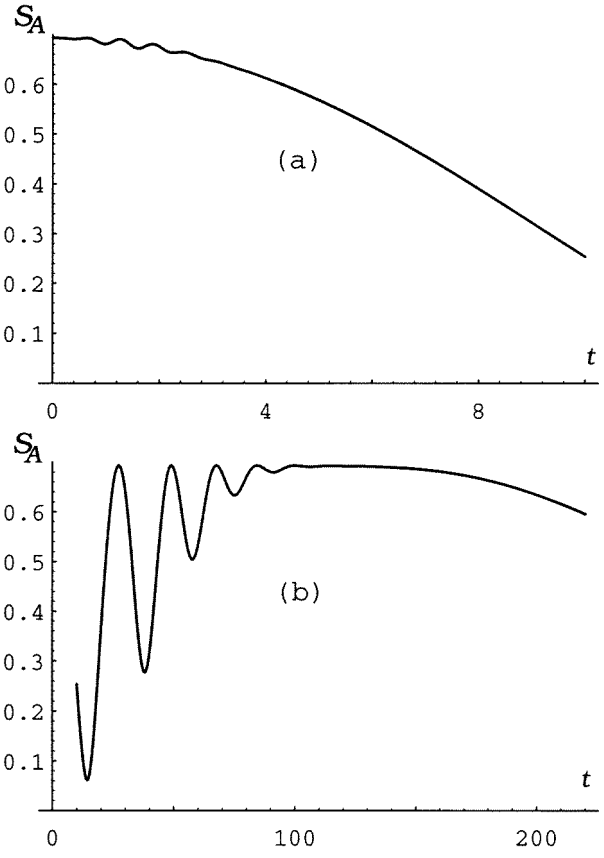

Figure 6. Time evolution of von Neumann entropy for $\rho_A = \frac{1}{2}\mathbb{1}_2$, $\alpha = 5$, $\kappa = 0.01$, and $\gamma = \Delta = 0$.

much from $\ln 2$, exactly as for the undamped case. Stage two can also be easily identified. The increase in κ has compressed its dynamics. The third minimum has moved from time $t \approx 75$ for figure 5(b) to time $t \approx 57$. For stage three the difference from figure 5(c) is huge. As κ is increased from 0.001 onwards, the plateau of maximum entropy becomes shorter and shorter, until at $\kappa = 0.01$ it has almost ceased to exist. Only on the interval $111 \leqslant t \leqslant 124$ the inequality $\ln 2 - S_A(t)/k_B < 10^{-3}$ is satisfied.

Since a small part of the third stage is still there, the smooth decay of the fourth stage does not come as a surprise. Here a compression of the dynamics has taken place, which is entirely due to the increase in damping. Measuring the time in units of κ^{-1}, we find that for both figures 5 and 6 the entropy needs a time of 9.0 units to reach the value of 10^{-3}. For our Markovian reference process a decrease in entropy from $\ln 2$ to 10^{-3} is found to take up an interval of duration $8.5\gamma_{\|}^{-1}$. We have made the choice $\xi(0)_{11} = \frac{1}{2}$ and $\xi(\infty)_{11} = 0$. Finally, the plots of the inversion, corresponding to figure 6, are omitted because this function evolves in a very simple manner. The value of $d(t)$ lies in the close vicinity of zero up to time $t = 83$, and subsequently decays to $-\frac{1}{2}$.

From the findings of figures 5 and 6 one can learn something about the evolution of small dissipative quantum systems. We recall that for α^2 sufficiently large the two-level atom undergoes an evolution of collapse and revival of Rabi oscillations, which possesses a strongly non-Markovian character and may be called quasireversible [15]. A substantial part of this evolution takes place on the interval $t < 4\sqrt{2}\alpha^2$; as discussed in the appendix, the bound is given by the collapse time belonging to the slow revival dynamics at zero damping parameter. For times of order κ^{-1} the Markovian damping term (4) becomes important, and the atom undergoes an irreversible decay to the ground state. In the case in which inequality $4\sqrt{2}\alpha^2 \ll \kappa^{-1}$ is satisfied, the two afore-mentioned timescales are well separated, so that one can study a crossover between two different kinds of dynamics. This is precisely what has been done in figure 5. Product $4\sqrt{2}\kappa\alpha^2$ takes on the value of 0.14 in that case.

Analysis of our plots and numerical data brings us to the following statement on dissipative behaviour of small quantum systems at zero temperature: during a transition from non-Markovian to Markovian evolution the state of maximum entropy may act as an attractor in phase space, rather than the state of minimum energy. Inside the phase space, which belongs to the two-level atom of the Jaynes–Cummings model, all trajectories converge at the central state. Subsequently, they follow a unique path to the ground state, given by $\frac{1}{2}(\mathbb{1}_2 + \lambda i_- - \lambda i_+)$, with $0 \leqslant \lambda \leqslant 1$. We emphasize that one may not look upon the central state as being an attractor in phase space for all times smaller than κ^{-1}; the trajectory corresponding to figure 6 starts at the central state, and passes through an almost pure state already at time $t \approx 15$. We should also mention that the remarkable role of the central state does not depend on the choice of initial condition for the field mode. If we replace in the parameter set of figure 5 the coherent state by a number state with 25 photons, then hardly anything happens to stages three and four. The plateau of maximum entropy now runs from $t = 54$ to $t = 1293$, and during its exponential decay the entropy reaches the value of 10^{-3} at $t = 10\,286$.

Once more we point out that the above-described crossover does not take place for all parameter choices. If α^2 lies between 10 and 25, and κ exceeds the value of 0.1, then one observes in the atomic entropy an abrupt change from oscillatory behaviour to smooth decay. If α becomes of order unity, then oscillations in entropy may persist throughout the whole atomic evolution. In all of these cases the ground state i_- acts as an attractor in phase space. The central state no longer possesses a special status.

Figure 7 provides a good illustration of the foregoing remarks. We have investigated

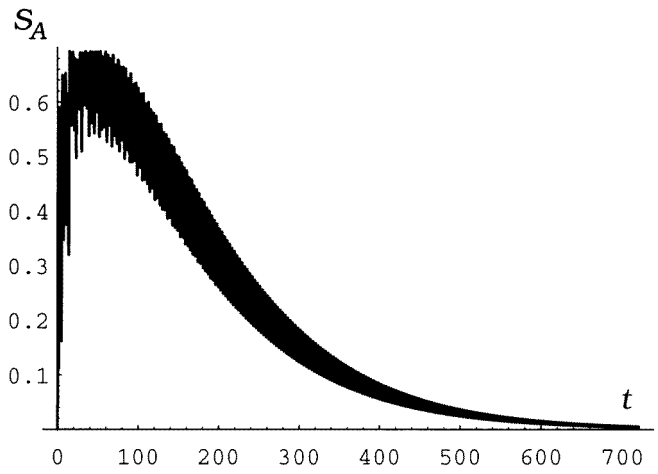

Figure 7. Asymptotic time evolution of von Neumann entropy for $\rho_A = i_+$, $\alpha = 1$, $\kappa = 0.01$, and $\gamma = \Delta = 0$.

the evolution of the entropy for $\alpha = 1$ and $\kappa = 0.01$; the atom starts from the excited state. For small times the entropy fluctuates in an irregular manner, thereby staying above the value of 0.5 on the interval $20 \leqslant t \leqslant 80$. As t becomes larger than 100 dissipation forces the entropy to converge to zero. However, instead of being monotonic the character of the decay is now oscillatory. One thus can say that for all times the dynamics is of a non-Markovian type. This assertion is confirmed by looking at the influence of the initial density matrix. Replacement of $\rho_A = i_+$ by $\rho_A = \frac{1}{2}\mathbb{1}_2$ does not affect the rate at which $S_A(t)$ decreases, but does suppress all oscillations of figure 7. Quantitatively speaking, we find that measure $\psi(200, 700)/k_B^2$ decreases from 0.49 for $\rho_A = i_+$ to the small value of 0.006 for $\rho_A = \frac{1}{2}\mathbb{1}_2$; these figures differ by a factor of about 80.

We conclude this section with a brief study of the dependence of measure ψ on cavity damping. We have evaluated the forms $\psi(0, T_d)$ and $\psi(T_d, \infty)$ for $\rho_A = i_+$, $\alpha = 5$, $\gamma = \Delta = 0$, and κ running from 0.001 to 1; for this choice of parameters the evolution of the entropy can be divided into a non-Markovian segment of oscillatory character and a Markovian segment of monotonic character. We call T_d the time at which the Markovian decay sets in. From a comparison between tables 1 and 2 one sees that even a modest cavity damping of $\kappa = 0.001$ causes a major decrease in entropy fluctuations. The value of measure $\psi(0, T_d)/k_B^2$ is more than 10 times smaller than the variation of entropy found for the second revival of Rabi oscillations at zero damping. As κ runs through the interval $[0.001, 1]$ measure $\psi(0, T_d)/k_B^2$ shrinks by a factor of 2 only, so for moderate to strong damping its dependence on κ may be called weak. In contrast, measure $\psi(T_d, \infty)$ increases linearly with the strength of cavity damping, if κ varies between 0.001 and 0.1. Such a behaviour does not puzzle us, in view of the fact that for our Markovian reference case ψ has been found to be proportional to damping parameter $\gamma_\parallel$. Altogether, measure ψ turns out to be an excellent tool for discriminating Markovian processes from non-Markovian ones.

Table 2. Values of measure ψ/k_B^2 for the non-Markovian and the Markovian parts of the atomic evolution. These correspond to the intervals $0 \leqslant t \leqslant T_d$ and $T_d \leqslant t \leqslant \infty$, respectively. The atom starts from state i_+; the other parameters are given by $\alpha = 5$ and $\gamma = \Delta = 0$.

κ	T_d	$\psi(0, T_d)/k_B^2$	$\psi(T_d, \infty)/k_B^2$
10^{-3}	1.05×10^3	1.02	1.1×10^{-4}
10^{-2}	1.23×10^2	0.77	1.1×10^{-3}
10^{-1}	2.03×10	0.74	1.1×10^{-2}
1	1.44	0.48	1.9×10^{-1}

4. Conclusion

Density matrix $\rho_A(t)$ as determined by master equation (1) represents an attractive model for studying the dynamics of small dissipative quantum systems. On the one hand the model can be solved exactly, and on the other hand it offers us a time evolution of a surprisingly high complexity. In the case in which the damping parameter κ equals zero the composite system of a two-level atom and privileged field mode undergoes a unitary time evolution. If the field is in a coherent state $|\alpha\rangle$ initially, the evolution of the two-level atom is governed by collapses and revivals of both slow and fast oscillations. The atom and field never stop exchanging energy, so convergence to a final state does not take place.

The picture becomes different as soon as we couple the field mode to a Markovian reservoir by choosing κ to be finite. Now the revival dynamics gives way to a regime of decay after a time of order κ^{-1}, so for all choices of parameters the atom ends up in its ground state. Under certain circumstances, for instance, if inequalities $10 \leqslant \alpha^2 \leqslant 25$ and $0.0001 \leqslant \kappa \leqslant 0.01$ are satisfied, the last part of each trajectory in atomic phase space is unique. All trajectories converge at the central state $\frac{1}{2}\mathbb{1}_2$; from there they follow the same path to the atomic ground state as for the process of spontaneous emission. Thus, not the ground state but rather the state of maximum entropy acts as the principal attractor in phase space.

We have put considerable effort in exploring the behaviour of quantity $S_A(t) = -k_B \operatorname{Tr}\{\rho_A(t) \ln \rho_A(t)\}$, the von Neumann entropy of the atom. Two aims have been achieved. First, we have demonstrated that function $S_A(t)$ is very well suited for characterizing the nature and strength of the interaction between the atom and field mode in a quantitative manner. This task has been carried out by measuring variations in entropy with the help of quantity ψ, defined in (24). It tells us to what extent the atom feels the presence of the field mode and Markovian reservoir during a certain time span.

It appears that for the undamped Jaynes–Cummings model measure ψ evolves in a nonmonotonic fashion. For α equal to 5 and 10 fluctuations in entropy are strongest not during the first but during the third and fifth revivals of the Rabi oscillations, respectively. Furthermore, the magnitude of ψ may depend a lot on the initial atomic state. In the damped case huge variations can be recorded even for times of order κ^{-1}. Such memory effects are nonexistent for Markovian processes. In other words, measure ψ may serve as an indicator for non-Markovian dynamics. We recall that for the process of spontaneous emission the form ψ has been evaluated analytically, so a solid Markovian reference case is available.

With our entropy studies we have also achieved something else. One may ask the fundamental question whether there exists a quantum counterpart of the second law of thermodynamics, valid for any irreversible quantum process. The damped Jaynes–Cummings model unites irreversibility with exemplary non-Markovian dynamics. Therefore,

the findings presented in section 3 permit us to assess the difficulties that must be overcome in extending formula (22) for entropy production. We have seen that the evolution of the entropy can be oscillatory, with two different timescales involved. As a consequence, for the dynamics of section 3 the time derivative in (22) will change its sign very frequently. We have to decide whether an extended formula for entropy production is to yield a positive result for all times.

A further difficulty to be faced concerns invariant states. The derivation of (22) rests on the assumption that only one such state exists. Obviously, our entropy plots as well as limits (29) and (30) undermine this assumption. What one could do as a first step toward an improved understanding of entropy production, is investigate the behaviour of formula (22) and related proposals [34] for an evolution that is a simplified version of the dynamics encountered in section 3. This might give us some clues as to how rigorous results on entropy production should look like outside the framework of semigroup-induced time evolution.

Acknowledgment

AJvW would like to thank the Swiss National Science Foundation for financial support.

Appendix. The atomic density matrix for large coherence parameter

Assuming that the field is in a coherent state $|\alpha\rangle$ at time zero, we evaluate the atomic density matrix for real and large coherence parameter α. The saddle-point method will be employed. We consider the undamped case, and set the detuning parameter equal to zero. In contrast to series (11), the results of this appendix can be easily interpreted. They enable the reader to develop a thorough understanding of how the dynamics of collapse and revival works. A similar treatment of (11) can be found in [35].

Use of Stirling's expansion paves the way for replacing in (11) all summations by integrations. This yields integrals of the following type

$$\int_{\epsilon}^{\infty} \mathrm{d}x\, h_i(x) \exp[-\alpha^2 g_i(x)] \tag{A1}$$

with $i = 1, 2$. Cut-off parameter ϵ ensures that the integrand is finite over the complete integration interval. One proves [25] that all summations in (11) decay exponentially fast for large α if the summation index n is kept smaller than $[\epsilon\alpha^2]$, and ϵ is sufficiently close to zero.

In leading order of α one finds

$$\begin{aligned} g_1(x) &= x \ln x - x + 2\mathrm{i}t\alpha^{-1}x^{1/2} \\ g_2(x) &= x \ln x - x - \mathrm{i}t\alpha^{-3}x^{-1/2}/2. \end{aligned} \tag{A2}$$

Since the function $\ln z$ is multivalued for complex z, there exist infinitely many saddle points $z = u(t)$ at each fixed time. One easily recognizes that not the time t but rather the phase $\arg u(t)$ is the natural parameter if it comes to specifying the results for integrals (A1).

For large α the atomic density matrix comes out as

$$\begin{aligned}
\rho_A(t)_{11} &= \tfrac{1}{2} + \mathrm{Re}\sum_{k=0}^{\infty}(-1)^{k+1}\mathcal{A}_1[(-1)^{k+1}\phi_k]\exp[-\alpha^2\Gamma_1(\phi_k) - \mathrm{i}(-1)^k\alpha^2\Omega_1(\phi_k)] \\
\rho_A(t)_{12} &= \mathrm{iIm}\sum_{k=0}^{\infty}(-1)^k\mathcal{A}_2[(-1)^{k+1}\phi_k]\exp[-\alpha^2\Gamma_1(\phi_k) - \mathrm{i}(-1)^k\alpha^2\Omega_1(\phi_k)] \\
&\quad +\mathrm{iIm}\sum_{k=0}^{\infty}(-1)^k\mathcal{A}_3[(-1)^{k+1}\chi_k]\exp[-\alpha^2\Gamma_2(\chi_k) - \mathrm{i}(-1)^k\alpha^2\Omega_2(\chi_k)] \\
&\quad +\mathrm{Re}\sum_{k=0}^{\infty}(-1)^k\mathcal{A}_4[(-1)^{k+1}\chi_k]\exp[-\alpha^2\Gamma_2(\chi_k) - \mathrm{i}(-1)^k\alpha^2\Omega_2(\chi_k)].
\end{aligned} \tag{A3}$$

Damping parameters $\{\Gamma_i\}$, frequencies $\{\Omega_i\}$, and amplitudes $\{\mathcal{A}_i\}$ are given by

$$\begin{aligned}
\Gamma_1(x) &= 1 - \exp[2x\tan x][\cos(2x) - 2x\tan x] \\
\Gamma_2(x) &= 1 - \exp[\tfrac{2}{3}x\tan x][\cos(\tfrac{2}{3}x) - 2x\sin(\tfrac{1}{3}x)\cos^{-1}(x)] \\
\Omega_1(x) &= \exp[2x\tan x][\sin(2x) + 2x] \\
\Omega_2(x) &= \exp[\tfrac{2}{3}x\tan x][\sin(\tfrac{2}{3}x) - 2x\cos(\tfrac{1}{3}x)\cos^{-1}(x)] \\
\mathcal{A}_1(x) &= \frac{1}{2}[(1+x\tan x)^2 + x^2]^{-1/4}\exp\left[-\frac{\mathrm{i}}{2}\arg(1+x\tan x+\mathrm{i}x)\right] \\
&\quad \times\{-\rho_{A,11} + \exp[-2x\tan x - 2\mathrm{i}x]\rho_{A,22} + 2\mathrm{i}\exp[-x\tan x - \mathrm{i}x]\mathrm{Im}\,\rho_{A,12}\} \\
\mathcal{A}_2(x) &= \frac{1}{2}[(1+x\tan x)^2 + x^2]^{-1/4}\exp\left[-x\tan x - \mathrm{i}x - \frac{\mathrm{i}}{2}\arg(1+x\tan x+\mathrm{i}x)\right] \\
&\quad \times\{-\rho_{A,11} + \exp[-2x\tan x - 2\mathrm{i}x]\rho_{A,22} + 2\mathrm{i}\exp[-x\tan x - \mathrm{i}x]\mathrm{Im}\,\rho_{A,12}\} \\
\mathcal{A}_3(x) &= \frac{1}{2}[(1+x\tan x)^2 + x^2]^{-1/4}\exp\left[-\frac{1}{3}x\tan x - \frac{\mathrm{i}}{3}x - \frac{\mathrm{i}}{2}\arg(1+x\tan x+\mathrm{i}x)\right] \\
&\quad \times\left\{-\rho_{A,11} - \exp\left[-\frac{2}{3}x\tan x - \frac{2\mathrm{i}}{3}x\right]\rho_{A,22}\right\} \\
\mathcal{A}_4(x) &= [(1+x\tan x)^2 + x^2]^{-1/4} \\
&\quad \times\exp\left[-\frac{2}{3}x\tan x - \frac{2\mathrm{i}}{3}x - \frac{\mathrm{i}}{2}\arg(1+x\tan x+\mathrm{i}x)\right]\mathrm{Re}\,\rho_{A,12}.
\end{aligned} \tag{A4}$$

The phases $\{\phi_k\}$ and $\{\chi_k\}$ must obey the following inequalities

$$0 \leqslant \phi_0, \chi_0 < \pi/2 \qquad (-\tfrac{1}{2}+k)\pi < \phi_k < (\tfrac{1}{2}+k)\pi \qquad (-\tfrac{1}{2}+3k)\pi < \chi_k < (\tfrac{1}{2}+3k)\pi \tag{A5}$$

with $k = 1, 2, 3, \ldots$. For each non-negative k there is a one-to-one correspondence between time $t \in (0, \infty)$ and phases (ϕ_k, χ_k), given by

$$\frac{t}{2\alpha} = \tau(\phi_k) \qquad \frac{3t}{8\alpha^3} = \tau(\chi_k). \tag{A6}$$

The function

$$\tau(x) = \left|\frac{x}{\cos x}\right|\exp(x\tan x) \tag{A7}$$

is monotonic on each interval specified under (A5).

For $i = 1, 2$ one proves that on a fixed interval (A5) damping parameter Γ_i possesses precisely one minimum and no maxima. The minima are given by $\Gamma_1(\phi_k = k\pi) = 0$ and

$\Gamma_2(\chi_k = 3k\pi) = 0$, with integer k non-negative. Upon substituting $\phi_k = k\pi + \epsilon$ and $\chi_k = 3k\pi + \epsilon$ in (A4), (A6), and (A7), and retaining leading orders in ϵ only, we arrive at

$$\begin{aligned} \alpha^2\Gamma_1 &= \tfrac{1}{2}(1 + k^2\pi^2)^{-1}(t - 2k\pi\alpha)^2 \qquad \alpha^2\Omega_1 = 2\alpha t - 2k\pi\alpha^2 \\ \alpha^2\Gamma_2 &= \tfrac{1}{32}\alpha^{-4}(1 + 9k^2\pi^2)^{-1}(t - 8k\pi\alpha^3)^2 \qquad \alpha^2\Omega_2 = -\tfrac{1}{2}\alpha^{-1}t - 2k\pi\alpha^2. \end{aligned} \tag{A8}$$

Obviously, the contributions in (A3) containing phase χ_k relate to the slow revival dynamics, whereas those containing phase ϕ_k relate to the fast revival dynamics. The terms with summation index $k = 1, 2, 3, \ldots$ generate the two kth revivals; from (A8) one finds the slow and fast revival times as $8k\pi\alpha^3$ and $2k\pi\alpha$, respectively. The terms with $k = 0$ describe the two collapses, with the slow and fast collapse times being equal to $4\sqrt{2}\alpha^2$ and $\sqrt{2}$, respectively. Finally, note that for $k = 0$ the imaginary part of factor $\exp[-\mathrm{i}\alpha^2\Omega_2]$ becomes zero at all revival times of the fast dynamics. This explains why in figure 1 each revival of Rabi oscillations coincides with a maximum in entropy.

All of the above results are valid under the condition that α be large. Numerical tests demonstrate that for $\alpha^2 \geqslant 25$ agreement between (A3) and the exact result (11) is very good.

References

[1] Agarwal G S 1973 *Progress in Optics* vol XI, ed E Wolf (Amsterdam: North-Holland) p 1
Haake F 1973 *Springer Tracts in Modern Physics* vol 66, ed G Höhler (Berlin: Springer) p 98
Louisell W H 1973 *Quantum Statistical Properties of Radiation* (New York: Wiley)
[2] Davies E B 1976 *Quantum Theory of Open Systems* (London: Academic) p 154
[3] von Neumann J 1927 *Gött. Nachr. Heft* **3** 273
[4] Ochs W 1975 *Rep. Math. Phys.* **8** 109
[5] Jaynes E T 1957 *Phys. Rev.* **106** 620
Jaynes E T 1957 *Phys. Rev.* **108** 171
[6] Wehrl A 1978 *Rev. Mod. Phys.* **50** 221
[7] Lindblad G 1983 *Non-equilibrium Entropy and Irreversibility* (Dordrecht: Reidel)
[8] Ohya M and Petz D 1993 *Quantum Entropy and its Use* (Berlin: Springer)
[9] de Groot S R and Mazur P 1962 *Non-equilibrium Thermodynamics* (Amsterdam: North-Holland) p 20
[10] Ananthakrishna G, Sudarshan E C G and Gorini V 1975 *Rep. Math. Phys.* **8** 25
[11] Spohn H 1978 *J. Math. Phys.* **19** 1227
[12] Brinati J R, Mizrahi S S and Prataviera G A 1994 *Phys. Rev.* A **50** 3304
[13] Davies E B 1973 *Commun. Math. Phys.* **33** 171
Davies E B 1974 *Commun. Math. Phys.* **39** 91
Davies E B 1976 *Math. Ann.* **219** 147
[14] Alicki R and Lendi K 1987 *Lecture Notes in Physics* vol 286, ed W Beiglböck (Berlin: Springer)
Davies E B 1980 *One-parameter Semigroups* (London: Academic)
[15] Eberly J H, Narozhny N B and Sanchez-Mondragon J J 1980 *Phys. Rev. Lett.* **44** 1323
[16] Jaynes E T and Cummings F W 1963 *Proc. Inst. Electr. Eng.* **51** 89
[17] Shore B W and Knight P L 1993 *J. Mod. Opt.* **40** 1195
[18] Aravind P K and Hirschfelder J O 1984 *J. Phys. Chem.* **88** 4788
[19] Phoenix S J D and Knight P L 1988 *Ann. Phys., NY* **186** 381
[20] Gea-Banacloche J 1990 *Phys. Rev. Lett.* **65** 3385
[21] Bužek V, Moya-Cessa H, Knight P L and Phoenix S J D 1992 *Phys. Rev.* A **45** 8190
[22] Aliskenderov E I, Ho Trung Dung and Knöll L 1993 *Phys. Rev.* A **48** 1604
[23] Knöll L and Orłowski A 1995 *Phys. Rev.* A **51** 1622
[24] Orszag M, Retamal J C and Saavedra C 1992 *Phys. Rev.* A **45** 2118
[25] van Wonderen A J 1997 *Phys. Rev.* A **56** 3116
[26] Gorini V, Frigerio A, Verri M, Kossakowski A and Sudarshan E C G 1978 *Rep. Math. Phys.* **13** 149
[27] Stenholm S 1973 *Phys. Rep.* **6** 1
[28] Narozhny N B, Sanchez-Mondragon J J and Eberly J H 1981 *Phys. Rev.* A **23** 236
[29] Lindblad G 1975 *Commun. Math. Phys.* **40** 147

[30] Gradshteyn I S and Ryzhik I M 1965 *Table of Integrals, Series, and Products* 4th edn (London: Academic) p 205
[31] Mao-Fa Fang and Guang-Hui Zhou 1994 *Phys. Lett.* A **184** 397
[32] Araki H and Lieb E 1970 *Commun. Math. Phys.* **18** 160
[33] Phoenix S J D and Knight P L 1991 *Phys. Rev.* A **44** 6023
[34] Lendi K, Farhadmotamed F and van Wonderen A J to be published
[35] Fleischhauer M and Schleich W P 1993 *Phys. Rev.* A **47** 4258